Microsc. Microanal. Microstruct. **6** (1995) 149–157 FEBRUARY **1995**, PAGE 149

Classification
Physics Abstracts
61.80J — 61.16D

In Situ EELS and TEM Observation of Boron Carbide (B_4C) During Hydrogen- and Helium-Ion Bombardments

Kouhei N. Kushita([1]), Kiichi Hojou([2]) and Shigemi Furuno([2])

([1]) Department of Radioisotopes, Japan Atomic Energy Research Institute Tokai-mura, Naka-gun, Ibaraki-ken, 319-11, Japan

([2]) Department of Materials Science and Technology, Japan Atomic Energy Research Institute Tokai-mura, Naka-gun, Ibaraki-ken, 319-11, Japan

(Received July 27, 1994; accepted January 3, 1995)

Abstract. — Increasing attention has been paid recently to boron carbide (B_4C) from a viewpoint of plasma-facing materials in a fusion device. This paper reports structural change of B_4C observed *in situ* by EELS and TEM during hydrogen- and helium-ion bombardments at room temperature. The B_4C became amorphous by the ion bombardments. This amorphization process was presented as a function of the shift of plasmon-loss peak energy and the change of core-loss profiles in addition to electron diffraction patterns. Analysis of core-loss peaks for boron as well as for carbon in B_4C during amorphization process revealed the formation of sp^2 type bonding between constituent carbon atoms by the ion bombardments.

1. Introduction

Boron carbide (B_4C) has been used in conventional nuclear reactors as neutron absorber due to the high cross section of B by the nuclear reaction of $^{10}B(n, \alpha)^7Li$. The B_4C also attracts a lot of attention for the use as the first-wall material in a fusion device because of its favorable nuclear properties to suppress plasma impurities [1, 2]. From these viewpoints, many kinds of studies have been carried out on the irradiation effects of neutron- [3, 4], hydrogen- [5], electron- [6], and helium-ion irradiations [7] on this material. There are few data, however, with electron energy-loss spectroscopy (EELS) on B_4C, the information from which is expected to help us understand the chemical aspect of the structural change of particle-bombarded B_4C.

Previously, we have carried out EELS studies on ion-bombarded graphite and diamond [8-10], in which EELS technique was found highly valid to study the change of chemical structure of the ion-bombarded materials.

This paper reports the results of *in situ* EELS and TEM observations of B_4C during hydrogen- and helium-ion bombardments. The EELS profiles changed along with crystalline-to-amorphous (C – A) transition of B_4C during ion bombardments. The C – A transition with its chemical aspect is discussed with respect to the changes of plasmon-loss peak and core-loss edge profiles.

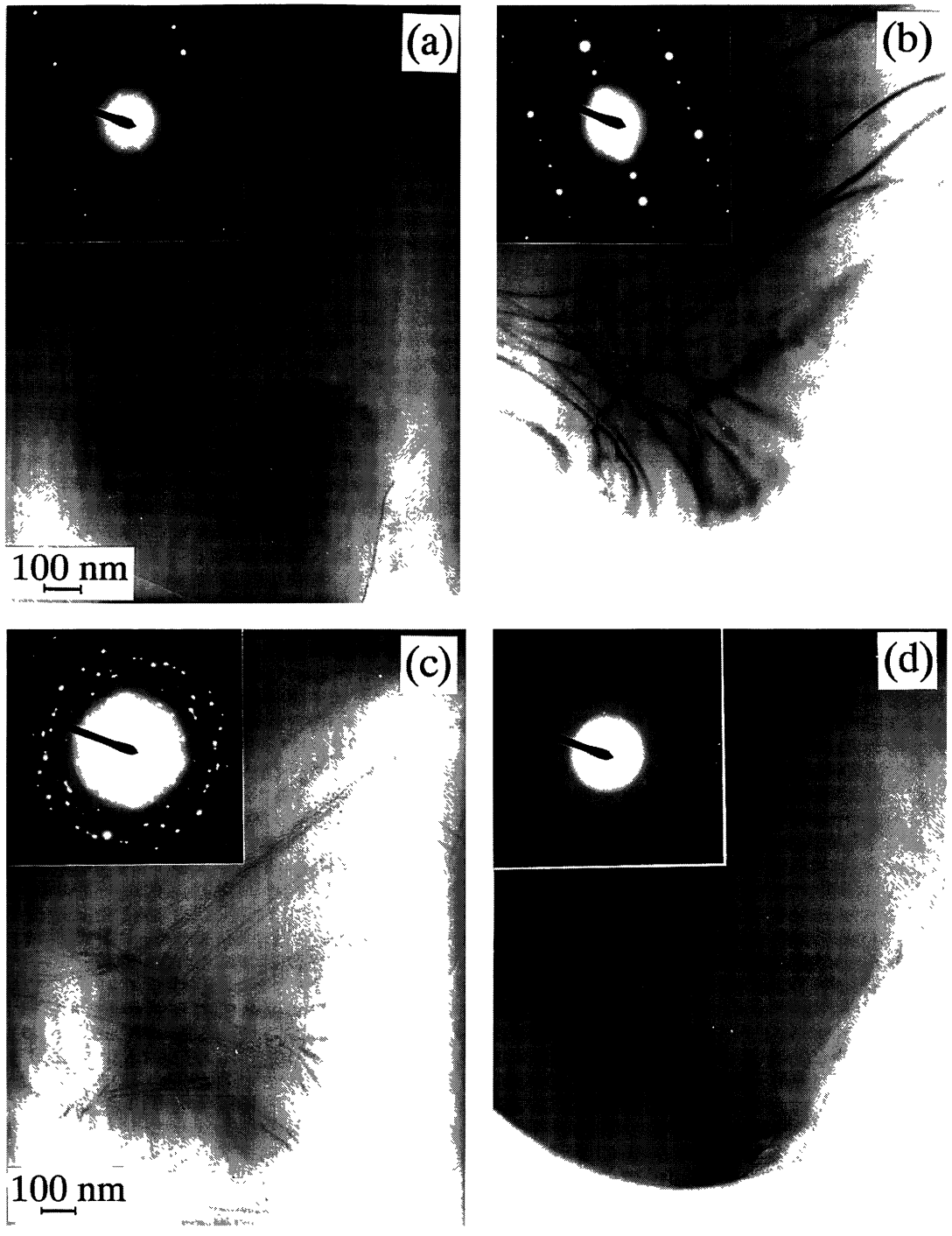

Fig. 1. — TEM images and selected-area electron diffraction patterns of B_4C bombarded with 16 keV H_2^+ ions; a) non-bombarded, b) 1.2×10^{17} $(H^+)/cm^2$, c) 3.6×10^{17} $(H^+)/cm^2$, d) 1.6×10^{18} $(H^+)/cm^2$.

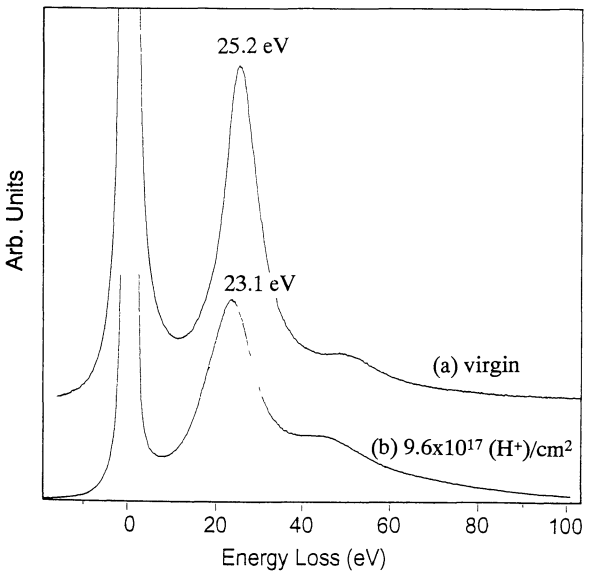

Fig. 2. — Comparison of plasmon-loss peak profiles of B_4C before and after hydrogen-ion bombardment.

2. Experimental

The original B_4C samples ($10 \times 10 \times 0.3$ mm, supplied from Furuuti Chem. Co. Ltd., Tokyo) were cut out into 3 mm⌀ discs and mechanically thinned by a dimpling machine, then further ion-etched by 2 keV Ar^+ beam for transmission electron microscopy (TEM) observations. The analytical electron microscope used in this study consisted of 400 keV TEM (JEOL-4000FX) equipped with a parallel-EELS (GATAN-666) and two ion guns. TEM observations were concluded at 200 keV, while the resolution of the p-EELS was about 1 eV. The B_4C samples were bombarded *in situ* in the electron microscope with 16 keV H_2^+ ions at room temperature at a flux of 2×10^{14} $(H^+)/cm^2$ s. For the experiments of hydrogen and helium double-ion bombardments, 12 keV He^+ (flux: 1×10^{14} $(He^+)/cm^2$ s) ions and 16 keV H_2^+ (flux: 1×10^{14} (H^+) $0/cm^2$ s) ions were employed so that the penetration depth in B_4C of both ion species was the same (average 82 nm). The total flux in the double-ion bombardment experiments was then 2×10^{14} ions/cm^2 s, the same as that of single ion bombardments of hydrogen. The ion beams were incident on the target at an angle of 30 degrees from the perpendicular axis of the sample surface.

3. Results and Discussion

For TEM and EELS observations, a small area of the sample with good crystalinity and suitable thickness was selected, as shown in Figure 1a. B_4C samples became amorphous when bombarded with hydrogen ions, and accordingly the Bragg spots in a selected-area electron diffraction (SAED) pattern became diffused and finally changed to a halo pattern, as shown in the inserts in Figure 1b to d. A change of the extinction contour lines in Figure 1 also indicates the amorphization process of the material.

In the case of hydrogen-ion bombardments, bubble formation was not obvious even after long-time bombardments as seen in Figure 1d. On the other hand, TEM images of B_4C bombarded

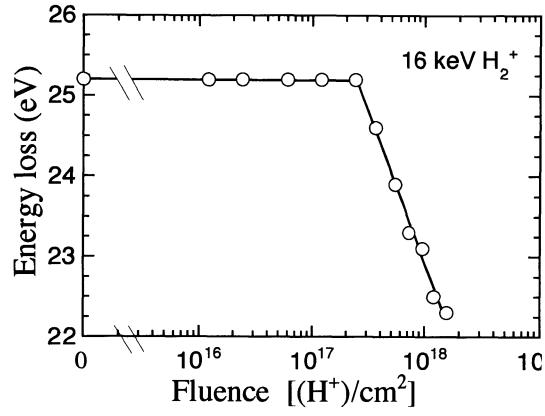

Fig. 3. — Change of plasmon-loss peak energy of B_4C bombarded with 16 keV H_2^+ ions.

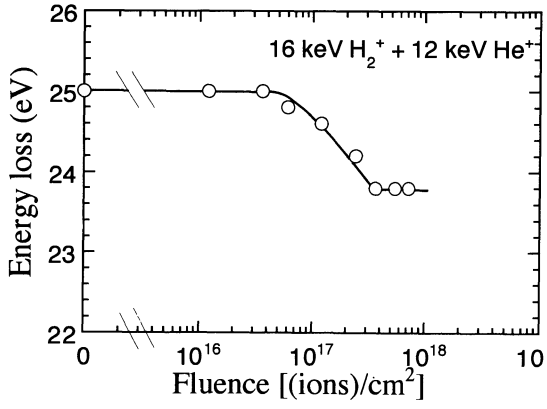

Fig. 4. — Change of plasmon-loss peak energy of B_4C bombarded simultaneously with 16 keV H_2^+ and 12 keV He^+ ions.

simultaneously with H_2^+ and He^+ ion showed small but observable bubbles, the phenomenon of which can be expected from reference data on helium-ion bombarded B_4C [7]. In the case of graphite [8, 11], bubbles are also more easily formed by helium-ion bombardments rather than hydrogen-ion bombardments. It is reported [12] that a part of hydrogen atoms implanted in highly-oriented pyrolytic graphite diffuse easily out of graphite by annealing, while the other part of hydrogen atoms are deeply trapped (possibly by forming C – H bonding) and do not easily released. Neither the deeply-trapped hydrogen nor the diffusing-out hydrogen atoms contribute bubble formation because these atoms do not easily aggregate to form bubbles. This interpretation may hold true for ion-bombarded B_4C. Helium atoms, on the other hand, do not form chemical bond and more easily trapped in voids during diffusion ending to form bubbles.

During the C – A transition of B_4C due to the hydrogen-ion bombardments, plasmon-loss peak of an EELS profile shifted to lower energy side as shown in Figure 2. Generally, the decrease of plasmon-loss peak energy implies the decrease of free- or valence-electron density in the material. In this case, the change of plasmon-loss peak energy is correspondent on the C – A

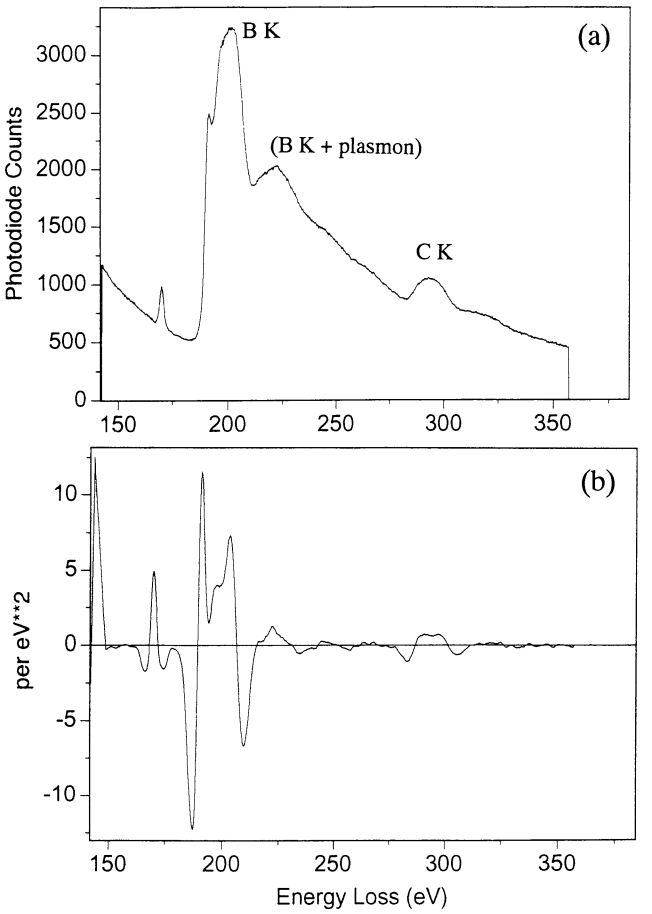

Fig. 5. — Core-loss EELS profile of virgin B_4C sample a), and its 2nd differential probile b).

transition of B_4C, as in the case of ion-bombarded graphite [8]. Figure 3 shows the relationship between hydrogen-ion fluence and plasmon-loss energy. It is clear that B_4C started to become amorphous with a threshold fluence of 2.5×10^{17} $(H^+)/cm^2$. In the case of simultaneous double-ion bombardment of H_2^+ and He^+ ions, the decrease of the plasmon-loss peak energy started about 4×10^{16} $(H^+)/cm^2$ as shown in Figure 4, earlier than the case of H_2^+ single ion bombardments. This discrepancy is reasonable considering the higher efficiency of helium ions than hydrogen ions to displace boron/carbon atoms in B_4C. Different ion flux may give different threshold fluence for C – A transition, though we cannot argue unambiguously at present. It has been reported [11] that the threshold fluence for C – A transition of graphite is a function of dpa (displacements per atom) and sample temperature during ion bombardments. One can expect, then, that different ion flux will cause different sample temperature, giving different threshold fluence for C – A transition of B_4.

It is also interesting to pay attention to the change of core-loss peaks in EELS profiles. In the core-loss profile of a virgin B_4C, as in Figure 5a, B K and C K edge peaks are seen at about 200 and 290 eV, respectively. It is noteworthy that a shoulder at about 285 eV became observable

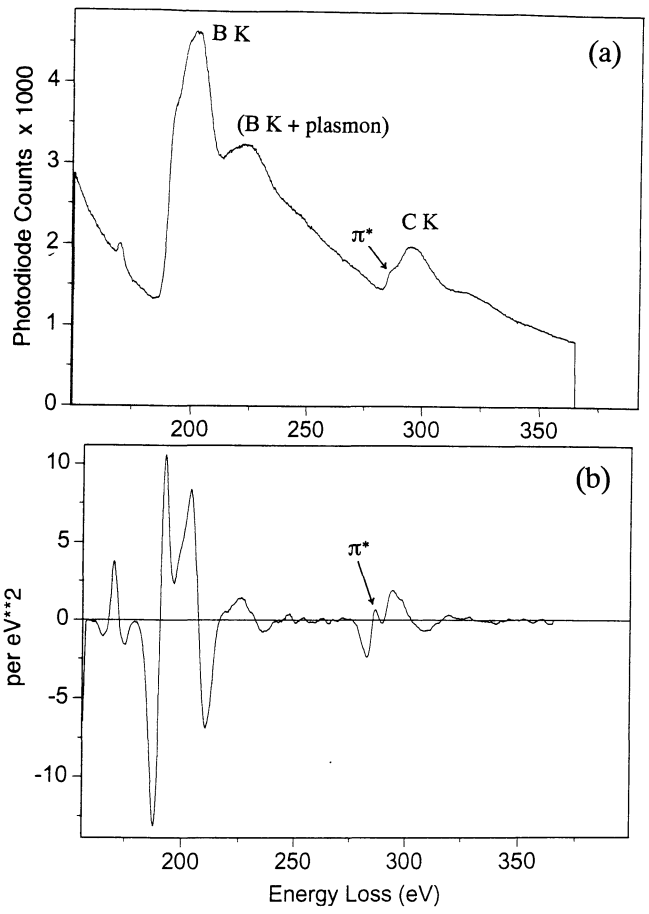

Fig. 6. — Core-loss EELS profile of B_4C bombarded with 16 keV H_2^+ ions to the fluence of 9.6×10^{17} $(H^+)/cm^2$ a), and its 2nd differential profile b).

after hydrogen bombardments as shown in Figure 6a. This phenomenon was also observed for B_4C bombarded simultaneously with hydrogen- and helium-ions (Fig. 7), and is more obvious in the second differential schemes of the core-loss profiles, as presented in Figure 6b and Figure 7b. This peak at 285 eV corresponds to π^* of C K edge. This π^* peak generally indicates the existence of sp^2 bonding, i.e., C = C double bonding in the material. This π^* peak have been observed even for amorphous graphite transformed by ion-bombardments, not only for crystalline graphite, indicating the existence of sp^2 carbon atoms, or C = C double bonding [8] in the amorphous carbon. Because the π^* peak appeared both for B_4C bombarded with single (H_2^+) ion species and with double (H_2^+ and He^+) ion species, as seen in Figure 6 and Figure 7, it is reasonable to think that the C = C double bonding has been produced by the displacements and rearrangement of constituent carbon atoms.

The core-loss peak profiles for boron, on the other hand, showed little fundamental change after ion bombardments. Then it is considered that the chemical state of boron atoms has been maintained almost the same as before, although the orientation of B – B and B – C bonding has become less ordered in amorphous B_4C.

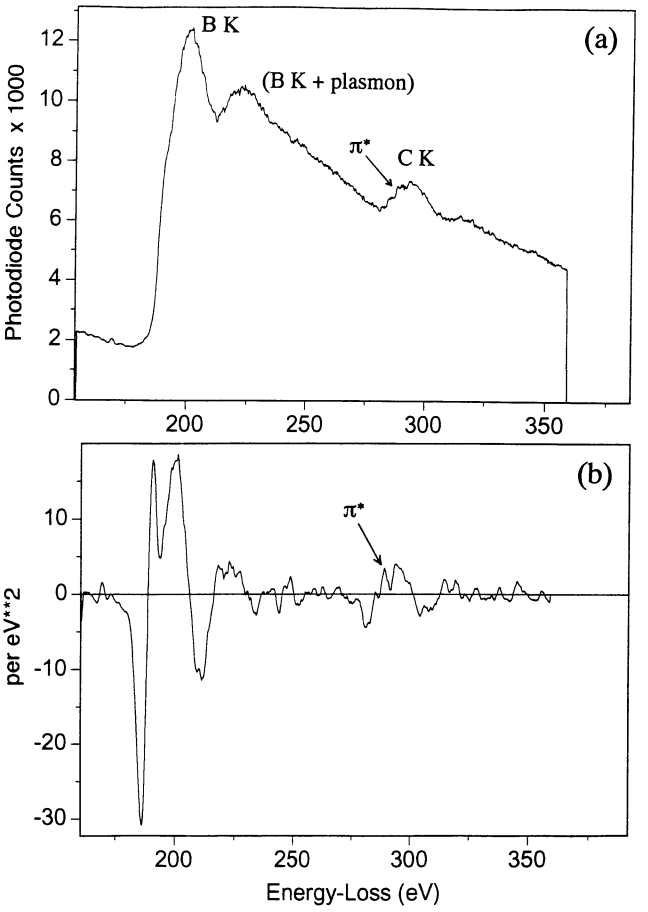

Fig. 7. — Core-loss EELS profile of B_4C bombarded simultaneously with 16 keV H_2^+ and 12 keV He^+ ions to the total fluence of 7.2×10^{17} (ions)/cm^2 a), and its 2nd differential profile b).

The amorphization processes of B_4C and graphite [8], represented by the change of plasmon-loss peak energies, are superimposed in Figure 8. This comparison suggests that B_4C is more resistant to amorphization by ion bombardments than graphite. By comparing double-ion (H_2^+ and He^+) bombardments with single-ion (H_2^+) bombardments, the former case was more effective on the amorphization of B_4C than the latter when the ion energies provided the same effective penetration depth. The plasmon-loss peak energy (25.2 eV) for virgin B_4C is lower than that (27.4 eV) of graphite, as seen in Figure 8, and much lower than that (35.6 eV) of diamond [9], which indicates that the valence-electron density of B_4C is lower than those of graphite and diamond.

Although the final plasmon-loss peak energies of ion-bombarded B_4C were not very reproducible, as they were dependent on the sample thickness and bombarding conditions, hydrogen-ion bombarded B_4C ended in much lower plasmon-loss peak energy than the others. Generally a – C : H (hydrogenerated amorphous carbon) shows lower plasmon-loss peak energy than that of amorphous graphite containing no hydrogen atoms. In addition to this tendency, a fact that hydrogen atoms in B_4C can be effectively expelled by helium-ion bombardments [13], seems to explain the above discrepancy.

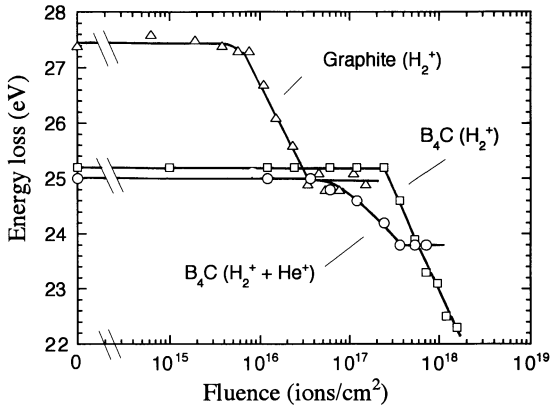

Fig. 8. — Change of plasmon-loss peak energy of graphite and B_4C bombarded with H_2^+ (and He^+) ions at the same total-ion flux at room temperature.

4. Conclusion

Amorphization process of B_4C was observed *in situ* by EELS and TEM during hydrogen- and helium-ion bombardments at room temperature. Bubble formation was hardly observed in B_4C bombarded with hydrogen ions, while small bubbles were observed when bombarbed simultaneously with hydrogen and helium ions. The plots of plasmon-loss peak energy *vs.* ion fluence made it possible to understand quantitatively the amorphization process of B_4C, and especially to identify a threshold fluence for the C – A transition.

Analysis of core-loss profiles of ion-bombarded B_4C indicated the formation of sp^2 type bonding between constituent carbon atoms. The formation of the C = C bonding was ascribed to the displacements and rearrangements of carbon atoms in B_4C due to ion bombardments.

Comparison of EELS profiles for B_4C and for graphite suggested higher resistance of B_4C than graphite to amorphization induced by ion bombardments. It was also shown that helium ions were more effective than hydrogen ions on the amorphization of B_4C.

References

[1] Dylla H.F., Bell M.G., Hawryluk R.J. *et al.*, *J. Nucl. Mater.* **176-177** (1990) 337-342.
[2] Saidoh M., Hiratsuka H., Arai T., Neyatani Y., Shimada M. and Koike T., *Fusion Eng. Des.* **22** (1993) 271-275.
[3] Jostsons A., Dubose C.K.H., Copeland G.L. and Stiegler J.O., *J. Nucl. Mater.* **49** (1973-74) 136-150.
[4] Hollenberg G.W. and Basmajan J.A., *J. Amer. Ceram. Soc.* **65** (1982) 179.
[5] Roth J., *J. Nucl. Mater.* **176-177** (1990) 132.
[6] Inui H., Mori H. and Fujita H., *Scripta Metall.* **22** (1988) 249-254.
[7] Stoto T., Ardonceau J. and Zuppiroli L., *Radiat. Eff.* **105** (1987) 17-30.
[8] Kushita K.N. and Hojou K., *Ultramicroscopy* **35** (1991) 289-293.
[9] Kushita K.N., Hojou K., Furuno S. and Otsu H., *J. Nucl. Mater.* **191-194** (1992) 346-350.
[10] Kushita K.N., Hojou K. and Furuno S., *J. Nucl. Mater.* **191-194** (1992) 351-355.

[11] Niwase K. and Tanabe T., *J. Nucl. Mater.* **179-181** (1991) 218-222.
[12] Kushita K.N., Youle I., Haasz A.A. and Sawicki J.A., *J. Nucl. Mater.* **179-181** (1991) 235-238.
[13] Yamauchi Y., Hirohata Y., Hino T., Yamashina T., Ando T. and Akiba M., Proc. of 11th Int. Conf. on Plasma Surface Interactions in Controlled Fusion Devices (PC24) (Mito, Japan, 1994).